

Composition from fast neutrons: application to the Moon

Olivier Gasnault¹, William C. Feldman¹, Sylvestre Maurice², Isabelle Genetay², Claude d'Uston³, Thomas H. Prettyman¹, and Kurt R. Moore¹

Abstract. Planetary neutron leakage fluxes provide a measure of surface composition. However to be used in geological studies, a quantitative relationship between measured fluxes and surface composition is needed. The present work shows that neutron production is expected to be a function of the atomic mass, and that the fast leakage flux in the energy range between 0.6 and 8 MeV is linearly related to the average soil atomic mass. This result is consistent with laboratory measurements, and with Lunar Prospector observations of the Moon. When calibrated with returned lunar samples, this relationship is used to construct a map of the average atomic mass of lunar soils.

Introduction

Important new measurements of lunar composition were made using Lunar Prospector (LP) instruments [Binder, 1998]. While gamma-ray spectroscopy gives information about the abundances of specific elements such as Th, Fe and Ti [Lawrence *et al.*, 2000; Prettyman *et al.*, 2001], neutron spectroscopy provides information about combinations of elements. Shapes of neutron energy spectra below ~ 500 keV are dominated by energy-loss and capture cross-sections for interactions between neutrons and the bulk chemical elements of the surface [Feldman *et al.*, 2000, and references therein]. In the following, we focus on measurements of neutrons above 600 keV, known as fast neutrons.

The lunar map of fast neutrons was measured using the Lunar Prospector Fast Neutron Spectrometer (LPFNS) between 0.6 and 8 MeV. Its comparison with the maps of albedo (at 750 nm) and of Fe demonstrates the sensitivity of fast neutrons to composition. Specifically, the fast neutron map shows a clear distinction between mare basalt terranes, which appear as strong fast neutron emitters, and the highlands, which appear as weak fast neutron emitters [Maurice *et al.*, 2000]. This map is so distinctive that it is important to develop a quantitative understanding of the information content of fast neutron fluxes to add to our geologic knowledge of the Moon.

The question of the chemical information content of fast neutron fluxes has been addressed by Gasnault *et al.* [2000], who confirmed the sensitivity of these fluxes to the presence of Fe and Ti in the soil. This sensitivity explains the main features of the fast neutron map from LP. Using computer

simulations, Gasnault *et al.* showed that leakage fluxes from the surface could be related to soil composition through a linear combination of weight fractions of each element in the near-surface soil. The coefficients given by Gasnault *et al.* were obtained by solving an over-determined system of simulated fast neutron fluxes, which introduces non-negligible uncertainties in the coefficients. In spite of these uncertainties, the published linear coefficients relating elemental weight fractions to leakage fluxes fit the simulations quite well. However, these same coefficients fail to reproduce the simulated relative fluxes from thick targets composed of only one element, and their relative values are not consistent with laboratory measurements of neutron yields from energetic particle bombardment of thick targets.

In this paper, we reinvestigate the relationship between the fast neutron leakage flux (energy between 0.6 and 8 MeV) and the composition of the lunar surface. We first generalize the results of a few laboratory experiments involving energetic proton thick-target neutron yields. Those experiments suggest a linear relationship between the fast neutron flux leaking from planetary surfaces and the average atomic mass of surface soils. A strong correlation between neutron production and the average atomic mass of surface soils is also found from an extensive set of Monte Carlo simulations. This result is confirmed by correlation between measured leakage fluxes using LPFNS and the atomic mass of lunar samples. We then use this correlation to construct a map of the average atomic mass of the lunar surface.

Neutron production in thick targets

Planetary neutrons are produced by interactions between Galactic Cosmic Rays (GCRs) and the nuclei of surface material. They result from two dominant types of nuclear reactions: knock-on/charge-exchange and spallation/evaporation. In the former case, the emerging neutrons have a range of energies that extend up to that of the incident proton. In the latter case, the distribution of neutron energies is a Maxwellian characterized by a temperature of several MeV.

For a thin target composed of a single element, it is possible to show that neutron production is proportional to the target mass. However, extrapolation to a thick target requires inclusion of neutron transport and a variety of multiple neutron production mechanisms that are not amenable to a simple analytical analysis. Numerical calculations supported by laboratory experiments are required to simulate this problem.

The ground-level measurements of neutron yield from thick targets of U, Pb, W and Sn irradiated by GCR protons at high-altitude made by Bercovitch *et al.* [1960] are one such example. These neutron yields increase with proton energy and with the atomic mass of the target, in agree-

¹Los Alamos National Lab., Los Alamos, New Mexico

²Observatoire Midi-Pyrénées, Toulouse, France

³Centre Etude Spatiale Rayonnements, Toulouse, France

ment with their Monte Carlo simulations of the nucleon cascade and subsequent neutron evaporation in the reactions. Other examples are the irradiations of thick targets of Be, Sn, Pb and U with accelerator-generated protons of 0.5 to 1.5 GeV [Fraser and Bartholomew, 1983]. Neutron yields from all targets except U were found to be a linear function of the incident proton energy, and a linear function of the atomic mass of the target. The result for U, which is a fissile material, showed a large increase in yield.

Using these laboratory results as a guide, we searched for a relationship between a parameter representative of the atomic mass of planetary soils and simulated fast neutron leakage fluxes. The most natural parameter is the average atomic mass, $\langle A \rangle$, of the soils. Quantitatively, $\langle A \rangle$ is given by an average over the number fraction times the atomic mass of each of the chemical elements in the soil:

$$\langle A \rangle = \sum_n f_n A_n = \frac{1}{\sum_n \omega_n / A_n}, \quad (1)$$

f_n is the number fraction of element n , A_n its atomic mass (in atomic mass units, amu), and ω_n its weight fraction.

Simulations of neutron production

In order to simulate the neutron yield from planetary surfaces exposed to GCRs, we developed a numerical code based on GEANT and GCALOR libraries [Brun et al., 1994; Zeitnitz and Gabriel, 1994] (see Gasnault et al. [2000], for a description of the modeling). The resultant code is quite reliable since results were successfully compared with measurements made using the LPFNS [Gasnault et al., 2000; Maurice et al., 2000].

Our code was used to simulate the neutron production, transport and leakage flux for the typical end-members of lunar minerals (anorthite and albite for the plagioclases, forsterite and fayalite for olivine, hedenbergite, diopside and enstatite for the pyroxenes, and ilmenite) and for the measured compositions of lunar samples (Apollo and Luna as tabulated in Haskin and Warren [1991]). First, we extract from the code the number of neutrons directly produced by

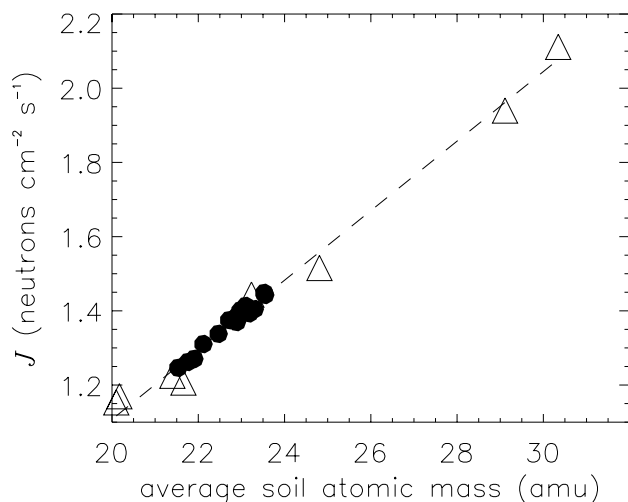


Figure 1. Simulated integrated neutron leakage flux from the lunar surface for typical lunar minerals (triangles) and typical lunar compositions (full circles). The integration is between 600 keV and 8 MeV.

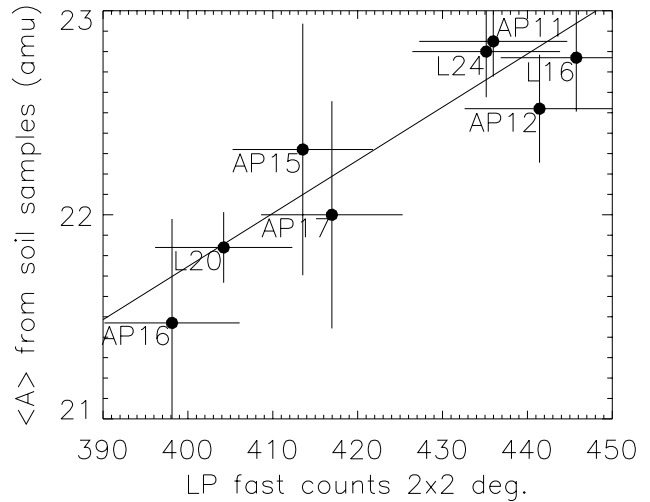


Figure 2. Average atomic mass of the sampled lunar soils versus fast neutron counts measured by Lunar Prospector in the landing site regions.

a GCR proton (hereafter called primary production). This task was implemented by surveying the full history of each GCR proton until it has lost all its kinetic energy (each proton can have several interactions and thus produce several primary neutrons). The results (not shown) reveal a very strong linear relation between the resultant neutron production and the corresponding $\langle A \rangle$ of the simulated compositions. These results are fit well by a straight line (correlation 0.997). Other simulations of soils that contain only one chemical element (from H to Pb, not shown here) also yield a very good linear relation, but with a lower slope. We speculate that the lower slope is caused by a mixing effect in the planetary composition simulations.

Simulations of neutron leakage flux

In order to simulate fast neutron leakage fluxes from planetary surfaces, we included secondary neutron production and transport. The transport of all secondary particles produced in the lunar surface has two effects. First, numerous new neutrons are produced, mainly by pions and high-energy primary neutrons, hereafter noted as secondary production. As for the primary neutron production, the secondary neutron production is found to be a linear function of $\langle A \rangle$ (not shown).

Second, subsequent collisions between all neutrons and the nuclear constituents of the planetary surface create an equilibrium spectrum of neutrons in energy as a function of depth. The fast neutron leakage flux is the fraction of this equilibrium neutron spectrum that escapes the surface to space, where they can be measured from orbit. Results for the same set of compositions chosen in the previous section are shown in Fig. 1. Inspection shows a strong linear relation between $\langle A \rangle$ and the simulated fast neutron leakage flux at the surface (correlation 0.994), given by:

$$J = a\langle A \rangle - b, \quad (2)$$

$$a = (94 \pm 2) \times 10^{-3}, \quad b = (77 \pm 4) \times 10^{-2},$$

$$\text{or inversely, } \langle A \rangle = cJ + d, \quad (3)$$

$$c = (10.6 \pm 0.3), \quad d = (8.3 \pm 0.4).$$

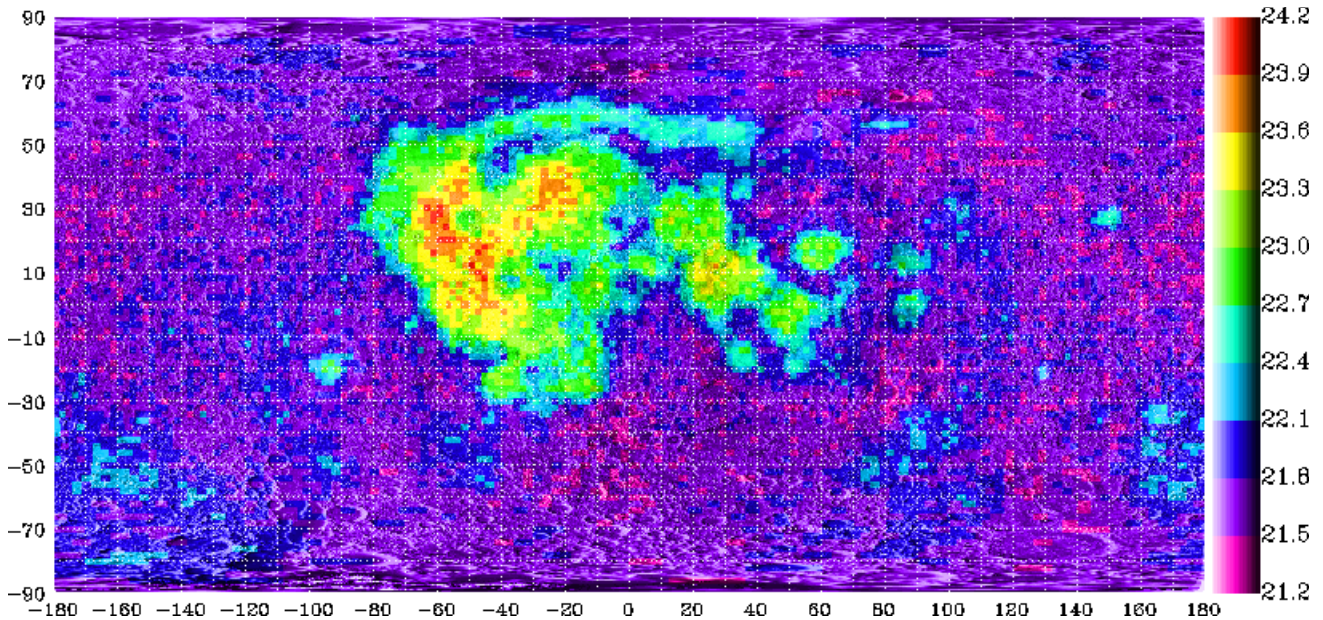


Plate 1. Map of the average atomic mass of the lunar surface in atomic mass unit. This is an equal area pixel distribution with a resolution of 60 km.

J is the neutron flux at the surface (neutrons $\text{cm}^{-2} \text{s}^{-1}$), and $\langle A \rangle$ is the average soil atomic mass (amu).

Note that (2) was obtained for our chosen energy spectrum of the GCR flux and holds only for typical mineral compositions; it may not be valid for soils having very small $\langle A \rangle$ (i.e. that contain light elements such as expected when water is abundant). Indeed J in (2) becomes negative when $\langle A \rangle < b/a = 8.2$ (note that $\langle A \rangle(\text{H}_2\text{O}) = 6$). Because hydrogen has both a strong reduced production and increased moderation effect on neutrons, its presence modifies (2) significantly; preliminary results show a decrease of the coefficient of $\langle A \rangle$ when $[\text{H}]$ increases, and it seems to be incorrect to use the coefficients a and b given in (2) when $[\text{H}]$ is above 0.1%. Other elements may also induce modifications of (2), depending on the binding energy of the “last neutron” in compound nuclei. But Fig. 1, as well as many other simulations (not shown), confirms that those modifications are small (except for hydrogen).

In summary, we believe that our present result is more robust than that obtained previously by Gasnault *et al.* [2000] for two main reasons: (a) the present coefficients are related to an actual nuclear parameter, the atomic mass, which is proven experimentally; and (b) the coefficients of the present relationship have lower uncertainties than those for the weight fraction coefficients obtained previously. Fast neutron spectroscopy can therefore be used to provide a measure of the average soil atomic mass of planetary surfaces through use of (2) or (3) when the soil is non-hydrogenous.

Atomic mass of lunar surface

The results of our simulations summarized by (2) and (3) are also globally supported by LPFNS observations. The fast neutron counting rates from the maria (which are rich in heavy elements such as Fe and Ti) are high, and those from the highlands (which are rich in lighter elements such as Al and Ca) are low [Maurice *et al.*, 2000]. Our present formulation is both consistent with, and an extension of the

conclusions reached by our previous studies, that fast neutrons are controlled by the abundances of Fe and Ti in lunar soils [Maurice *et al.*, 2000; Gasnault *et al.*, 2000]. Indeed, Fe and Ti are the most massive atoms of the major elements in lunar minerals, and their abundances are good markers of $\langle A \rangle$ of the various lunar terranes. It is thus not surprising that the fast neutron map from LP delineates the major terranes of the lunar surface.

The simulated results summarized by (2) and (3) can be checked by correlating LPFNS measurements with $\langle A \rangle$ of the various lunar soil samples. For this purpose, we use the fast neutron counts in each 2×2 degree spatial pixel from Maurice *et al.* [2000] that overlay each of the Apollo and Luna landing sites. The average atomic mass, $\langle A \rangle$, for each of these sites is calculated using data for “soils and regolith breccias” given in Table A8.1 of Haskin and Warren [1991]. The results are plotted in Fig. 2. The correlation line is given by:

$$\langle A \rangle = eC + f, \quad (4)$$

$$e = (26 \pm 6) \times 10^{-3}, \quad f = (11 \pm 3),$$

where C are the counts measured by LPFNS.

This result is consistent with our simulations (eq. (3)). Although there are mixing effects due to the relatively low spatial resolution of LPFNS, the correlation between C and $\langle A \rangle$ in Fig. 2 is very good (0.917). The offsets d and f are equal within their uncertainties given in (3) and (4), and the difference between the slopes c and e is explained by the instrumental response function of the LPFNS. The clear trend in Fig. 2 supports the simulation results shown in Fig. 1, which reveal that the fast neutron leakage flux is directly proportional to $\langle A \rangle$. Equation (4) can therefore be used to construct a map of the average atomic mass of the lunar surface from the measurements of LPFNS. The resulting map is given in Plate 1. It is identical to the fast neutron counts map presented by Maurice *et al.* [2000], but with a new absolute scale. The pixels in Plate 1 with the lowest $\langle A \rangle$ values

(about 21 amu) are scattered over the highlands, while those with the highest $\langle A \rangle$ values (about 24 amu) are concentrated at the west and south of the Aristarchus plateau. The uncertainties in the fit in (4) and in LPFNS counts (2%) lead to a standard deviation in $\langle A \rangle$ for this map of between 15% and 20%.

Conclusions

We have shown that a direct relation between the fast neutron flux and the atomic mass, suggested by laboratory measurements, is generally valid for cosmic ray induced fast leakage fluxes from planetary surfaces. We have derived a linear relationship for a wide range of lunar compositions, and have shown that a similar relation applies to fluxes observed by LPFNS above the Apollo and Luna landing sites. This observed relation was then used to construct a map of the average soil atomic mass of the lunar surface from measured LPFNS counting rates, with a precision of about 20%. The map delineates the various types of terranes that differ primarily in their Fe content. However, according to equation (4), the abundances of other major elements also contribute significantly. Those other elements (such as Ca and Al) will play an important role when [Fe] is low, i.e. in the highlands that cover most of the lunar surface. The map of the average soil atomic mass of the lunar surface therefore provides distinctive new information that will aid future studies of the Moon.

Acknowledgments. This work was supported by DOE (LA-UR-01-488) and NASA. The authors are thankful for the constructive remarks from the referees.

References

- Bercovitch, M., H. Carmichael, G. Hanna, and E. Hincks, Yield of neutrons per interaction in U, Pb, W and Sn by protons of six energies between 250 and 900 MeV selected from cosmic radiation, *Phys. Rev.*, *119*, 412-431, 1960.
- Binder, A.B., Lunar Prospector: Overview, *Science*, *281*, 1475-1476, 1998.
- Brun, R.F., F. Carminati, S. Giani, et al., GEANT detector description and simulation tool, *Program Library W5013*, Eur. Organ. For Nucl. Res., Geneva, 1994.
- Feldman, W.C., D.J. Lawrence, R.C. Elphic, D.T. Vaniman, D.R. Thomsen, and B.L. Barraclough, Chemical information content of lunar thermal and epithermal neutrons, *J. Geophys. Res.*, *105*, 20347-20363, 2000.
- Fraser, J.S. and G.A. Bartholomew, Spallation neutron sources, in *Neutron sources for basic physics and applications*, edited by S. Cierjacks, pp. 217-235, Oxford; New York: Pergamon Press, 1983.
- Gasnault, O., C. d'Uston, W.C. Feldman, and S. Maurice, Lunar fast neutron leakage flux calculation and its elemental abundance dependence, *J. Geophys. Res.*, *105*, 4263-4271, 2000.
- Haskin, L., and P. Warren, Lunar chemistry, in *Lunar source book, a user's guide to the Moon*, edited by G.H. Heiken, D.T. Vaniman, and B.M. French, pp. 357-474, Cambridge Univ. Press, 1991.
- Lawrence, D.J., W.C. Feldman, B.L. Barraclough, A.B. Binder, R.C. Elphic, S. Maurice, M.C. Miller, and T.H. Prettyman, Thorium abundances on the lunar surface, *J. Geophys. Res.*, *105*, 20307-20331, 2000.
- Maurice, S., W.C. Feldman, D.J. Lawrence, R.C. Elphic, O. Gasnault, C. d'Uston, I. Genetay, and P.G. Lucey, High-energy neutron from the Moon, *J. Geophys. Res.*, *105*, 20365-20375, 2000.
- Prettyman, T.H., W.C. Feldman, D.J. Lawrence, R.C. Elphic, O. Gasnault, S. Maurice, K.R. Moore, and A.B. Binder, Distribution of iron and titanium on the lunar surface from Lunar Prospector gamma-ray data, *Proc. Lunar Planet. Sci. Conf. 32nd, #2122* (CD-ROM), 2001.
- Zeitnitz, C. and T. Gabriel, The GEANT-CALOR interface and benchmark calculations of ZEUS test calorimeters, *Nucl. Instrum. Methods Phys. Res.*, *A349*, 106-111, 1994.
- W. Feldman, O. Gasnault, K. Moore, and T. Prettyman, Los Alamos National Laboratory, P.O. Box 1663, M.S. D466, Los Alamos, NM 87545. (e-mail: gasnault@lanl.gov)
- C. d'Uston, Centre d'Etude Spatiale des Rayonnements, 9 avenue Roche, B.P. 4346, 31028 Toulouse Cedex 4, France.
- I. Genetay, and S. Maurice, Observatoire Midi-Pyrénées, 14 avenue Edouard Belin, 31400 Toulouse, France.

(Received February 23, 2001; revised July 02, 2001; accepted July 11, 2001.)